Improved Inductance Identification Method Based on High Frequency Signal Characteristics Acquisition for IPMSM Considering Voltage Phase Delay

Zhiwei Chen, *Member, IEEE*, Chaoyang Geng, Yongpeng Shen, *Member, IEEE*, Mingjie Wang, and Xiaoliang Yang, *Member, IEEE*

***Abstract*—For the inductance identification method of interior permanent magnet synchronous motor based on high-frequency (HF) signal injection, the accuracy of HF response current and voltage information acquisition is the key to determine the inductance identification results. To improve the accuracy of inductance identification, this article proposes an inductance identification method based on the acquisition of HF response current and HF voltage characteristics. The method establishes an inductance identification matrix about HF voltage characteristics and HF current characteristics under the consideration of the effects of stator resistance and cross-coupling, and realizes the accurate acquisition of HF current characteristics by multimultiple rotational coordinate transformation in the ABC coordinate system. The mechanism of digital control delay on the injected HF voltage and sampled HF current is also analyzed, and a digital control delay compensation strategy for the HF voltage is proposed. Then, according to the obtained HF response current characteristics and HF voltage characteristics, which are substituted into the established inductance identification matrix, the online identification of inductance is realized. Finally, the feasibility and superiority of the proposed method are verified by experiment.**

***Index Terms*—Control delay, current characteristics, high frequency (HF) injection, inductive identification, interior permanent magnet synchronous motor (IPMSM).**

I. Introduction

INTERIOR permanent magnet synchronous motor (IPMSM) has the advantages of simple structure, high efficiency, high power density, etc., and is widely used in home appliances, electric vehicles, rail transportation and other fields and various control systems [1], [2]. With the development of industry, the performance requirements for motor control systems are undergoing sustained escalation, motor control strategies that meet the requirements of different performance indicators are constantly proposed. And the effectiveness of the implementation of each of these control strategies is affected by the motor parameters [3], [4]. How to realize the accurate identification of motor parameters has become the content of extensive research by scholars at home and abroad.

The rank-deficient is the biggest problem faced in motor parameter identification. Since the IPMSM steady-state voltage equation has a rank of 2, while IPMSM has four parameters for the motor: stator resistance, permanent magnet flux linkage, *dq*-axis inductance. Therefore, it is difficult to realize the full parameter identification of the motor based on the IPMSM steady state voltage equation. To solve the rank-deficient problem, a series of schemes have also emerged in recent years. These methods are mainly categorized into two types: the nonsignal injection based methods [5], [6], [7], [8], [9], [10], [11], [12], [13] and signal injection based methods [14], [15], [16], [17], [18], [19], [20], [21], [22], [23], [24], [25], [26], [27], [28], [29].

For the nonsignal injection method, Liu and Zhu [5] used a fixed part parameter approach, fixing one or several parameters of the motor to nominal or measured values, The full rank of the identification matrix is achieved by reducing the number of parameters that need to be identified in the voltage equation, However, the accuracy of parameter identification is heavily dependent on the accuracy of the fixed parameters. Rajia et al. [6] increases the rank of the discrimination matrix by setting different *d*-axis currents in order to introduce multiple sets of voltage equations. However, different currents cause changes in motor parameters. Therefore, such methods are also subject to certain identification errors. All of the above parameter identification methods rely on the steady-state mathematical model of the motor, Yu et al. [8] and [9] proposes to have full-parameter identifiability under the dynamic mathematical model of the motor and to increase the rank of the identification matrix by detecting the voltage and current information under the switching state of the inverter, thus realizing the full-parameter online identification of the motor, In order to realize current sampling at switching frequencies, high bandwidth current sensors such as Roche coils as well as differential circuits need to be added to the hardware circuit.

Received 7 January 2025; revised 6 March 2025; accepted 13 April 2025. Date of publication 16 April 2025; date of current version 30 June 2025. This work was supported in part by the National Natural Science Foundation of China General Program under Grant 62273313, in part by the Natural Science Foundation of Hennan Province under Grant 252300421572, in part by the Doctoral Research Fund of Zhengzhou University of Light Industry under Grant 2023BSJJ028, in part by the Science and Technology Key Project of Henan Province under Grant 242102240104 and Grant 242102221029, in part by the Henan Province Key R&D Project 241111242300, and in part by the Science and Technology Innovation Talent Support Plan in Universities of Henan Province under Grant 24HASTIT046. Recommended for publication by Associate Editor B. Singh. *(Corresponding author: Yongpeng Shen.)*

The authors are with the College of Electrical and Information Engineering, Zhengzhou University of Light Industry, Zhengzhou 450002, China (e-mail: chenzw@tju.edu.cn; 332301010016@zzuli.edu.cn; shenyongpeng@zzuli.edu.cn; mjwang@zzuli.edu.cn; yangxl@hnu.edu.cn).

Color versions of one or more figures in this article are available at https://doi.org/10.1109/TPEL.2025.3561462.

Digital Object Identifier 10.1109/TPEL.2025.3561462

The signal injection method is another effective method to increase the rank of the parameter identification matrix, which has received extensive attention from scholars in recent years. This method is used to obtain high frequency current or voltage information obtained by induction by injecting different forms of voltage or current signals into the motor, Since the motor high-frequency (HF) voltage equation contains the inductance, the information of the injected signal can be used to realize the identification of the inductance, and further combined with the fundamental wave voltage equation can realize the full parameter identification [14], [15], [16]. For the signal injection method, the accuracy of obtaining the HF voltage information and HF response current information acting on the motor end is a key factor affecting the accuracy of motor parameter identification [27], [28], [29]. From the point of view of the way of obtaining HF voltage information and HF response current information, the current signal injection method can be divided into two categories: one is aimed at obtaining HF information amplitude; the other is aimed at obtaining HF information amplitude and phase angle.

Kang et al. [19] and Yu and Wang [20] injected HF voltages into the motor, calculated the amplitude of the sinusoidal fundamental waveform voltage components at the same frequency, and combined with the inverter nonlinear voltage error compensation to obtain the HF voltage amplitude information. At the same time, on the basis of ignoring the stator resistance and cross-coupling terms, the positive and negative sequence HF current amplitude information is obtained by implementing the multi-frequency rotational coordinate transformation of the HF response current in the *dq* coordinate system. However, the neglect of the stator resistance and the cross-coupling term will inevitably cause some error.

To avoid the preceding problems, the injected HF sinusoidal voltage can obtain the real and imaginary part information of the HF voltage and HF response current in the *dq* coordinate system by compensating the injected HF sinusoidal voltage by the nonlinear voltage error of the inverter and combining with the discrete Fourier transform (DFT) to obtain the amplitude and phase angle of the HF information [22], [23], [24], [25]. Although this method can realize the amplitude and phase angle acquisition of HF information without neglecting the stator resistance, the DFT needs to process the current-voltage information in multiple control cycles, which makes the implementation process slightly complicated, and at the same time, the neglect of the cross-coupling term will also cause certain errors. In addition, the method needs to be to obtain the amplitude and phase angle, and the literature mentioned above only consider the effect of inverter nonlinearity on the voltage, and not consider the effect of the digital control delay on the HF voltage information, which is another important factor affecting the effect of the motor terminal voltage another important factor.

Based on the preceding analysis, how to accurately obtain HF voltage and current information is a very important task. Specific performance are as follows.

1) Research on accurate HF response current information acquisition method without neglecting stator resistance and cross-coupling terms.
2) The effect of digital control delay on HF ac voltage signals has remained to be analyzed, and the applicability of existing digital control delay compensation methods has to be further investigated.

Therefore, this article investigates the IPMSM inductance identification method based on HF signal injection. First, the implementation process and deficiencies of two currently existing methods for obtaining HF voltage and current information are analyzed, as well as their shortcomings. Then, the inductance identification matrices with respect to the HF voltage characteristics and the HF current characteristics are established, considering the effects of stator resistance and cross-coupling. Then, the accurate acquisition of HF current characteristics is realized with the multi-frequency rotational coordinate transformation in the ABC coordinate system. Meanwhile, the influence mechanism of the digital control delay on the injected HF voltage and the sampled HF current is analyzed, and the digital control delay compensation strategy for the HF voltage is proposed. Finally, according to the obtained HF response current and voltage characteristics, which are substituted into the established inductance identification matrix to realize the online identification of inductance. The feasibility and superiority of the proposed method are verified by experiments.

II. IPMSM Mathematical Model

The *dq*-axis voltage equation of IPMSM

$$\begin{cases} u_d = R_s i_d + L_d \frac{d}{dt} i_d - \omega_e L_q i_q \\ u_q = R_s i_q + L_q \frac{d}{dt} i_q + \omega_e (L_d i_d + \psi_f) \end{cases} \tag{1}$$

where u_d, u_q are the *dq*-axis components of stator voltage; i_d, i_q are the *dq*-axis components of stator current; R_s is the stator resistance; ω_e is the electrical angular velocity; L_d, L_q are the *dq*-axis inductance components; ψ_f represents the stator flux linkage of the permanent magnet.

The torque equation can be expressed as

$$T_e = \frac{3}{2} p_n i_q \left[i_d (L_d - L_q) + \psi_f \right] \tag{2}$$

where T_e is the electromagnetic torque and p_n is the number of rotor pole pairs.

After injecting a HF voltage signal to the IPMSM, the corresponding HF voltage equation can be expressed as

$$\begin{cases} u_{dh} = R_s i_{dh} + L_d p i_{dh} - \omega_e L_q i_{qh} \\ u_{qh} = R_s i_{qh} + L_q p i_{qh} - \omega_e L_d i_{dh} \end{cases}. \tag{3}$$

As can be seen from (3), the HF voltage equation contains inductive information, therefore, the HF voltage equations can be utilized to achieve the identification of the *dq*-axis inductance, and further combined with the fundamental wave voltage equations can achieve the full-parameter identification of the IPMSM [20]. The IPMSM inductance identification method based on HF signal injection is shown in Fig. 1.

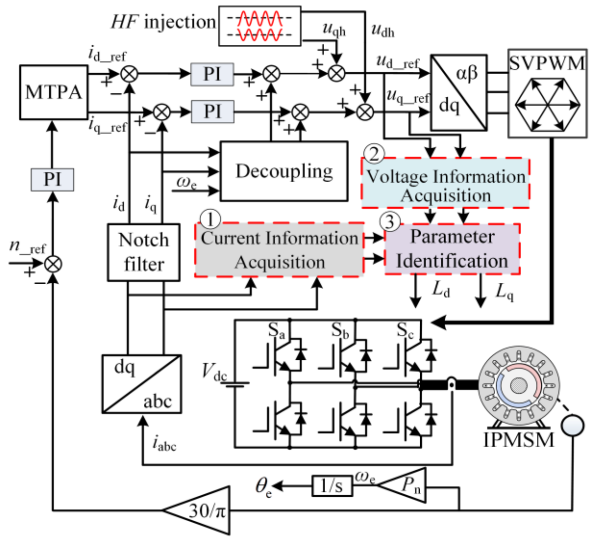

Fig. 1. IPMSM inductance identification based on HF signal injection.

III. Parameter Identification Based on HF Voltage and Current Information

At present, two methods of parameter identification based on HF voltage and current information are available: Parameter identification method based on the acquisition of HF signal amplitude information; and parameter identification method based on amplitude and phase acquisition of HF signals. Both methods are briefly analyzed as follows.

A. Parameter Identification Based on Amplitude Information of HF Signals

A pair of HF voltage signals u_{dqh} is injected into the IPMSM in d, q coordinate system. The injected HF voltage signal is represented in the form of a complex vector

$$\begin{aligned} \boldsymbol{u}_{dqh} &= u_{dh} + ju_{qh} \\ &= U_h \cos(\omega_h t) + jU_h \sin(\omega_h t) \\ &= U_h e^{j\omega_h t} \end{aligned} \tag{4}$$

where U_h is the amplitude of the HF voltage signal and ω_h is the frequency of the HF voltage signal.

Neglecting the stator resistance and cross-coupling terms, the IPMSM HF mathematical model is simplified as

$$\begin{cases} u_{dh} = L_d p i_{dh} \\ u_{qh} = L_q p i_{qh} \end{cases}. \tag{5}$$

By substituting (4) into (5), the d- and q-axis HF response currents can be obtained as

$$\begin{aligned} \boldsymbol{i}_{dqh} &= \frac{U_h}{L_d} \int \cos(\omega_h t) dt + j \frac{U_h}{L_d} \int \sin(\omega_h t) dt \\ &= \frac{U_h}{\omega_h L_d L_q} \left[L_\Sigma e^{j(\omega_h t - \frac{\pi}{2})} + L_\Delta e^{j(-\omega_h t + \frac{\pi}{2})} \right] \\ &= A_P e^{j(\omega_h t - \frac{\pi}{2})} + A_N e^{j(-\omega_h t + \frac{\pi}{2})} \end{aligned} \tag{6}$$

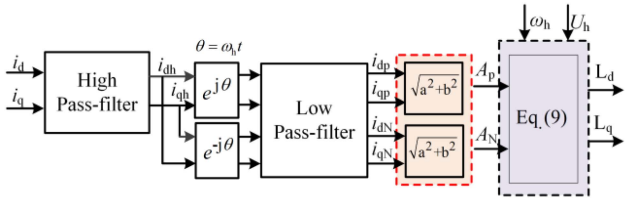

Fig. 2. Inductance parameter identification based on the acquisition of HF signal amplitude information.

where L_Σ and L_Δ are the average inductance and differential inductance; A_P and A_N represent the amplitude of the positive and negative sequence HF current components.

L_Σ and L_Δ can be expressed as

$$\begin{cases} L_\Sigma = 0.5(L_d + L_q) \\ L_\Delta = 0.5(L_d - L_q) \end{cases}. \tag{7}$$

A_P and A_N can be expressed as

$$\begin{cases} A_P = \frac{L_\Sigma U_h}{\omega_h L_d L_q} \\ A_N = \frac{L_\Delta U_h}{\omega_h L_d L_q} \end{cases}. \tag{8}$$

According to (8), the amplitude of the positive and negative sequence HF current components contains d- and q-axis inductance information. Therefore, inductance identification can be achieved by obtaining the positive and negative sequence components of the HF response current. Combining (7) and (8), the expression of the inductance with respect to the high frequency voltage and current amplitude information can be obtained

$$\begin{cases} L_d = \frac{U_h}{\omega_h (A_P - A_N)} \\ L_q = \frac{U_h}{w_h (A_P + A_N)} \end{cases}. \tag{9}$$

The extraction of the positive and negative sequence components of the HF response current can be achieved using the inverse Park transform and filter, and the structure of parameter identification based on the acquisition of HF signal amplitude information is shown in Fig. 2. The method utilizes a simplified HF mathematical model, and the neglect of the stator resistance as well as the cross-coupling term can cause incorrect identification models, which in turn can lead to errors in the identification inductance results.

B. Parameter Identification Based on Amplitude and Phase Acquisition of HF Signals

In order to avoid the problems of the methods described in Section III-A, recent studies have proposed parameter identification methods based on acquisition of amplitude and phase information from HF signals. The method realizes the simultaneous identification of L_d, L_q, and R_s by obtaining the amplitude and phase information of the HF signal.

Neglecting the cross-coupling term and representing the HF voltage and current information in sinusoidal form, the IPMSM

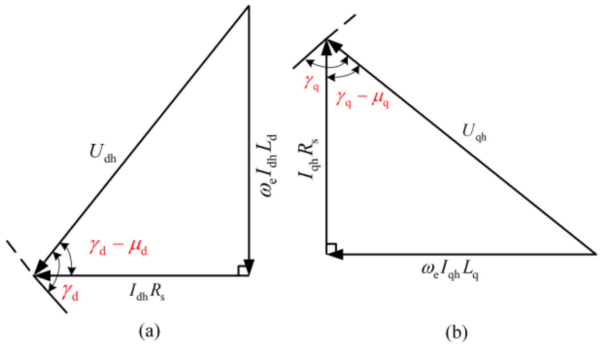

Fig. 3. Vector diagram of IPMSM HF equivalent impedance modeling. (a) Vector diagram of d-axis HF equivalent impedance model. (b) Vector diagram of q-axis HF equivalent impedance model.

HF voltage equation is represented as

$$\begin{cases} U_{dh}\sin(\omega_h t+\gamma_d) = R_s I_{dh}\sin(\omega_h t+\mu_d) \\ \quad +\omega_h L_d I_{dh}\sin(\omega_h t+\mu_d+\frac{\pi}{2}) \\ U_{qh}\sin(\omega_h t+\gamma_q) = R_s I_{qh}\sin(\omega_h t+\mu_q) \\ \quad +\omega_h L_q I_{qh}\sin(\omega_h t+\mu_q+\frac{\pi}{2}) \end{cases} \tag{10}$$

where U_{dh}, U_{qh}, I_{dh}, I_{qh} represent the HF voltage and current amplitude of d- and q-axis, respectively; and γ_{dh}, μ_{dh}, γ_{qh}, μ_{qh} represent the initial phase angles of the HF voltage and HF current in the d- and q-axis, respectively.

Expressing (12) as a HF equivalent impedance model of the form

$$\begin{cases} U_{dh}e^{j(\omega_h t+\gamma_d)} = R_s I_{dh}e^{j(\omega_h t+\mu_d)} \\ +\omega_e L_d I_{dh}e^{j(\omega_h t+\mu_d+\pi/2)} \\ U_{qh}e^{j(\omega_h t+\gamma_q)} = R_s I_{qh}e^{j(\omega_h t+\mu_q)} \\ +\omega_e L_q I_{qh}e^{j(\omega_h t+\mu_q+\pi/2)} \end{cases}. \tag{11}$$

The vector diagram of the dq-axis HF equivalent impedance model is shown in Fig. 3. The relationship between d- and q-axis inductances and stator resistance of the motor about the HF voltage, current amplitude and phase can be obtained from the figure.

$$\begin{cases} L_d = \frac{U_{dh}}{\omega_h I_{dh}}\sin(\gamma_d-\mu_d) \\ L_q = \frac{U_{qh}}{\omega_h I_{qh}}\sin(\gamma_q-\mu_q) \\ R_s = \frac{U_{xh}}{\omega_x I_{xh}}\cos(\gamma_x-\mu_x) x=d,q \end{cases}. \tag{12}$$

To obtain the HF voltage and current amplitude and phase, the DFT [22], [23] can be applied as follows:

$$\begin{cases} X_{\mathrm{Re}} = \frac{2}{N}\left[x_{dqh}(0)+\sum_{i=1}^{N-1} x_{\mathrm{dqh}}(i)\cos\frac{2\pi i}{N}\right] \\ X_{\mathrm{Im}} = \frac{2}{N}\left[-\sum_{i=1}^{N-1} x_{dqh}(i)\sin\frac{2\pi i}{N}\right] \\ X_{\mathrm{mag}} = \sqrt{{X_{\mathrm{Re}}}^2+{X_{\mathrm{Im}}}^2} \\ X = U, I \; x = u, i, N = 1, 2\cdots \end{cases} \tag{13}$$

where X_{Re} and X_{Im} are the real and imaginary components of the HF signal. X_{mag} is the amplitude of the HF signal.

According to the DFT, the HF voltage and current amplitude and phase can be expressed as

$$\begin{cases} U_{xh} = \sqrt{{U_{\mathrm{Re}}}^2+{U_{\mathrm{Im}}}^2} \\ \gamma_{xh} = \tan^{-1}(U_{\mathrm{Im}}/U_{\mathrm{Re}}) \\ I_{xh} = \sqrt{{I_{\mathrm{Re}}}^2+{I_{\mathrm{Im}}}^2} \\ \mu_{xh} = \tan^{-1}(I_{\mathrm{Im}}/I_{\mathrm{Re}}) x=d,q \end{cases}. \tag{14}$$

Finally, according to (12) and (14), the identification of d- and q-axis inductances and stator resistance can be realized.

The method improves the identification accuracy by obtaining the amplitude and phase of the HF signal and considering the effect of stator resistance. However, the following problems remain.

1) The effects of cross-coupling were not considered.
2) The effect of the digital control delay on the alternating current signal needs to be further analyzed.

IV. Proposed Multiparameter Identification Method Based on the Acquisition of HF Current Characteristics

In view of the preceding issues, this article proposes an inductance identification method based on the acquisition of HF response current and HF voltage characteristics. The method includes the following three main components.

1) Inductance identification matrix establishment based on HF signal characteristics.
2) Method of accurately obtaining HF current characteristics.
3) Analysis and compensation of the effect of digital control delay on HF signals.

A. Inductance Identification Matrix Based on HF Signal Characteristics

In the dq coordinate system, the HF current of the IPMSM and the HF voltage at the motor terminal can be expressed as

$$\begin{cases} i_{dh} = I_{dh}\cos(\omega_h t+\mu_d) \\ i_{qh} = I_{qh}\sin(\omega_h t+\mu_q) \end{cases} \tag{15}$$

$$\begin{cases} u_{dh} = U_{dh}\cos(\omega_h t+\gamma_d) \\ u_{qh} = U_{qh}\sin(\omega_h t+\gamma_q) \end{cases} \tag{16}$$

where U_{dh} and U_{qh} are the amplitude of HF voltage signals acting on the motor in the d- and q-axis; I_{dh}, I_{qh} are the amplitude of HF current signals induced by the motor; μ_d, μ_q, γ_d, γ_q are the initial phase angles injected into the HF currents and the HF voltage signals; and ω_h is the frequency of the HF voltage signals.

Substituting (15) and (16) into (3) obtains

$$\begin{cases} U_{dh}\cos(\omega_h t+\gamma_d) = R_s I_{dh} I_{dh}\cos(\omega_h t+\mu_d) \\ \quad -\omega_h L_d I_{dh}\sin(\omega_h t+\mu_d) - \omega_e L_q I_{qh}\sin(\omega_h t+\mu_q) \\ U_{qh}\cos(\omega_h t+\gamma_d) = R_s I_{qh} I_{qh}\sin(\omega_h t+\mu_d) \\ \quad +\omega_h L_q I_{qh}\sin(\omega_h t+\mu_q) + \omega_e L_d I_{dh}\sin(\omega_h t+\mu_d) \end{cases}. \tag{17}$$

Expanding (17) in terms of characteristics can be obtained as

$$\begin{cases} U_{dh}\cos\gamma_d = R_s I_{dh}\cos\mu_d - \omega_h L_d I_{dh}\sin\mu_d \\ -\omega_e L_q I_{qh}\sin\mu_q \\ U_{dh}\sin\gamma_d = R_s I_{dh}\sin\mu_d + \omega_h L_d I_{dh}\cos\mu_d \\ +\omega_e L_q I_{qh}\cos\mu_q \\ U_{qh}\cos\gamma_q = R_s I_{qh}\cos\mu_q - \omega_h L_q I_{qh}\sin\mu_q \\ -\omega_e L_d I_{dh}\sin\mu_d \\ U_{qh}\sin\gamma_q = R_s I_{qh}\sin\mu_q + \omega_h L_q I_{qh}\cos\mu_q \\ +\omega_e L_d I_{dh}\cos\mu_d \end{cases}. \tag{18}$$

As shown in (18), the HF voltage-current characteristics equation includes the stator resistance and the d-axis and q-axis inductances. Therefore, three of the characteristics equations can be used to realize the identification of the inductance. By rewriting (18) in the form of a matrix

$$\begin{bmatrix} U_{dh}\cos\gamma_d \\ U_{dh}\sin\gamma_d \\ U_{qh}\cos\gamma_q \\ U_{qh}\sin\gamma_q \end{bmatrix} = \begin{bmatrix} R_s & -\omega_h L_d & 0 & -\omega_e L_q \\ \omega_h L_d & R_s & \omega_e L_q & 0 \\ 0 & -\omega_e L_d & R_s & -\omega_h L_q \\ \omega_e L_d & 0 & \omega_h L_q & R_s \end{bmatrix} \times \begin{bmatrix} I_{dh}\cos\mu_d \\ I_{dh}\sin\mu_d \\ I_{qh}\cos\mu_q \\ I_{qh}\sin\mu_q \end{bmatrix}. \tag{19}$$

B. Method of Accurately Obtaining HF Current Characteristics

According to (19), the accuracy of the identification of the motor parameters depends on the precise determination of the HF voltage and HF response current characteristics. When a HF sinusoidal voltage signal as shown in (16) is injected in the dq coordinate system, the induced HF response current can be expressed as the form of (15) in the dq coordinate system. The expression of the HF response current in the $\alpha\beta$ coordinate system can be obtained by subjecting (15) to the IPARK transformation as follows:

$$\begin{cases} i_{\alpha h} = I_{h1}\cos[(\omega_e+\omega_h)t+\chi_1] \\ \quad\quad +I_{h2}\cos[(\omega_e-\omega_h)t+\chi_2] \\ i_{\beta h} = I_{h1}\sin[(\omega_e+\omega_h)t+\chi_1] \\ \quad\quad +I_{h2}\sin[(\omega_e-\omega_h)t+\chi_2] \end{cases} \tag{20}$$

where I_{h1}, I_{h2}, χ_1, and χ_2 are the amplitude and initial phase angle of the HF response currents with frequencies ω_e+ω_h and ω_e-ω_h.

At the same time, the relationship between them and the amplitude and initial phase angle of the HF response current in the dq-axis is as follows:

$$\begin{cases} I_{dh}\cos\mu_d = I_{h1}\cos\chi_1 + I_{h2}\cos\chi_2 \\ I_{qh}\cos\mu_q = I_{h1}\cos\chi_1 - I_{h2}\cos\chi_2 \\ I_{dh}\sin\mu_d = I_{h1}\sin\chi_1 - I_{h2}\sin\chi_2 \\ I_{qh}\sin\mu_q = I_{h1}\sin\chi_1 + I_{h2}\sin\chi_2 \end{cases}. \tag{21}$$

Therefore, the HF response current characteristics in the dq coordinate system can be further obtained by obtaining the HF response current characteristics in the $\alpha\beta$ coordinate system.

In order to obtain the HF response current characteristics in the $\alpha\beta$ coordinate system, the sample obtained $\alpha\beta$ currents

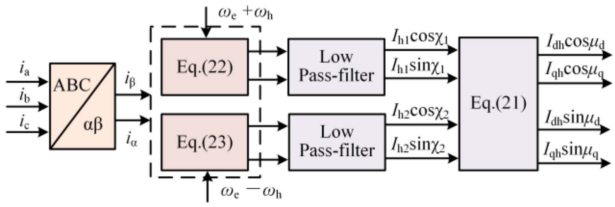

Fig. 4. Proposed high-frequency response current characteristics acquisition.

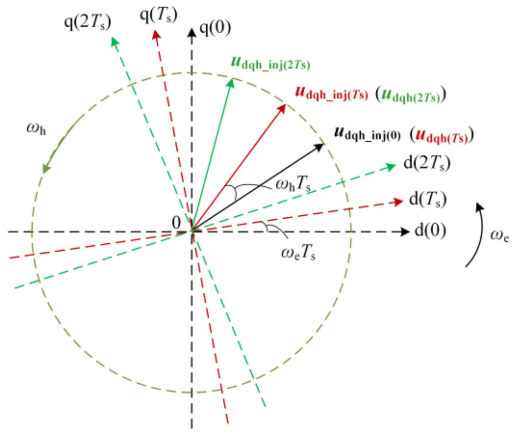

Fig. 5. HF voltage vector and synchronized rotating coordinate system changes in two continuous control cycles.

can be transformed by the multifrequency rotating coordinate transformation shown as

$$T_1 = \begin{bmatrix} \cos((\omega_e+\omega_h)t) & \sin((\omega_e+\omega_h)t) \\ -\sin((\omega_e+\omega_h)t & \cos((\omega_e+\omega_h)t) \end{bmatrix} \tag{22}$$

$$T_2 = \begin{bmatrix} \cos((\omega_e-\omega_h)t) & \sin((\omega_e-\omega_h)t) \\ -\sin((\omega_e-\omega_h)t & \cos((\omega_e-\omega_h)t) \end{bmatrix}. \tag{23}$$

Significantly, since the sampled motor currents contain not only HF response currents, but also fundamental and other frequency harmonics. Therefore, the motor current obtained from the sampling is passed through (22) and (23) to obtain an HF response current characteristics interspersed with a certain content of alternating current. In order to separate the HF response current characteristic quantities, a low-pass filter is also needed to be used. The proposed method for obtaining the HF response current characteristics is shown in Fig. 4.

C. Analysis of the Effect of Digital Control Delay on HF Signals and Compensation Methods

In addition to the inverter nonlinear voltage error, the digital control delay and the rotor position variation during one control cycle is another important factor that leads to the inconsistency between the output voltage of the d- and q-axis current controllers and the actual voltage applied to the motor terminal. If the following corrections are made to the output voltage of the current controller, the actual fundamental voltage added to the motor terminal and the fundamental voltage output by the

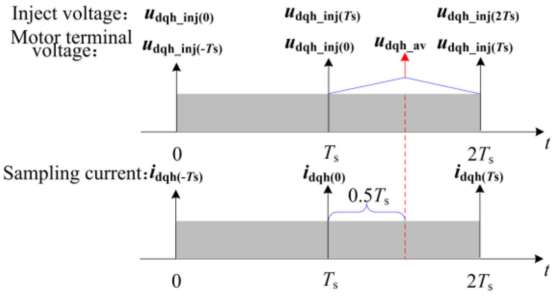

Fig. 6. Relationship between the HF current obtained from sampling at the moment of T_s and the HF response current produced by the motor when the average voltage vector acts.

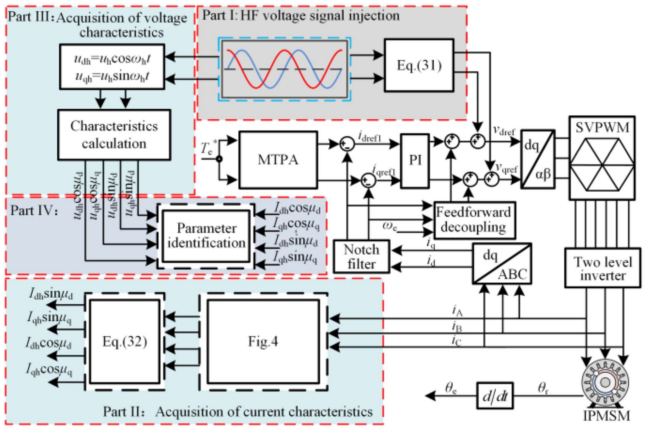

Fig. 7. Proposed inductance identification based on the acquisition of HF response current and HF voltage characteristics.

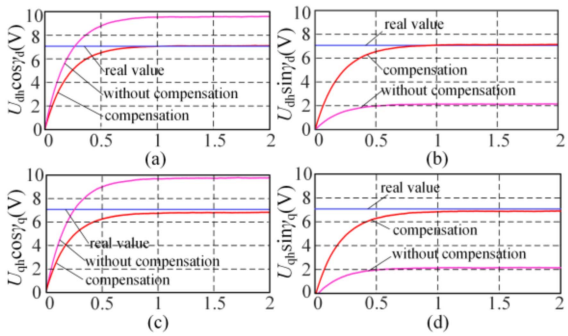

Fig. 8. Simulation results of HF voltage characteristics. (a) $U_{dh}\cos\gamma_d$. (b) $U_{dh}\sin\gamma_d$. (c) $U_{qh}\cos\gamma_q$. (d) $U_{qh}\sin\gamma_q$.

controller can be made consistent [30]

$$\begin{cases} u_{d\_\mathrm{com}} = m\left[u_{d\_c}\cos(1.5\omega_e T_s) - u_{q\_c}\sin(1.5\omega_e T_s)\right] \\ u_{q\_\mathrm{com}} = m\left[u_{d\_c}\sin(1.5\omega_e T_s) + u_{q\_c}\cos(1.5\omega_e T_s)\right] \end{cases} \tag{24}$$

$$m = \frac{\omega_e T_s}{2\sin(0.5\omega_e T_s)} \tag{25}$$

where u_{d_c} and u_{q_c} are the dq-axis voltages output from the controller; u_{d_com} and u_{q_com} are the corrected controller output voltages; and T_s is the control period.

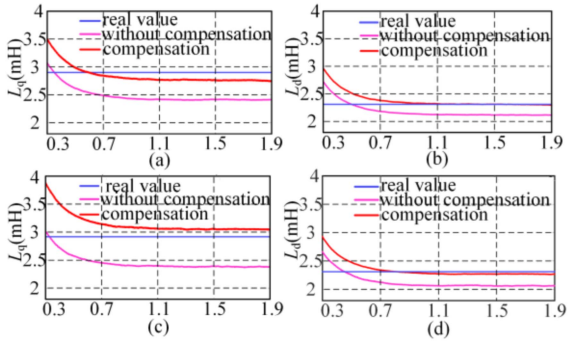

Fig. 9. Inductance identification results after and before compensation. (a) q-axis inductance at 200 r/min. (b) d-axis inductance at 200 r/min. (c) q-axis inductance at 1200 r/min.(d) d-axis inductance at 1200 r/min.

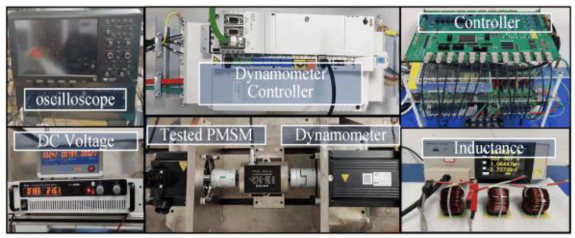

Fig. 10. Experimental system of permanent magnet synchronous motor.

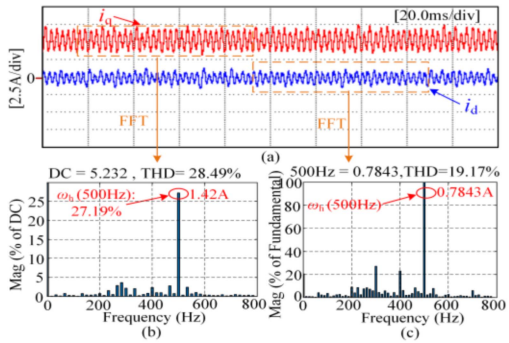

Fig. 11. dq-axis current waveform with FFT analysis. (a) dq-axis current waveform. (b) FFT analysis of HF current signals in d-axis. (c) FFT analysis of HF current signals in q-axis.

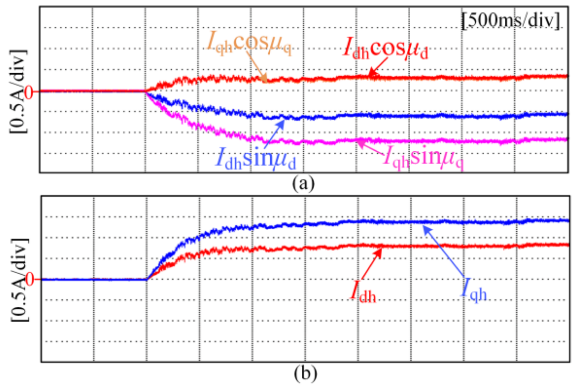

Fig. 12. Extracted HF current information waveforms. (a) Extracted dq-axis HF current characteristics results. (b) Extracted dq-axis HF current amplitude results.

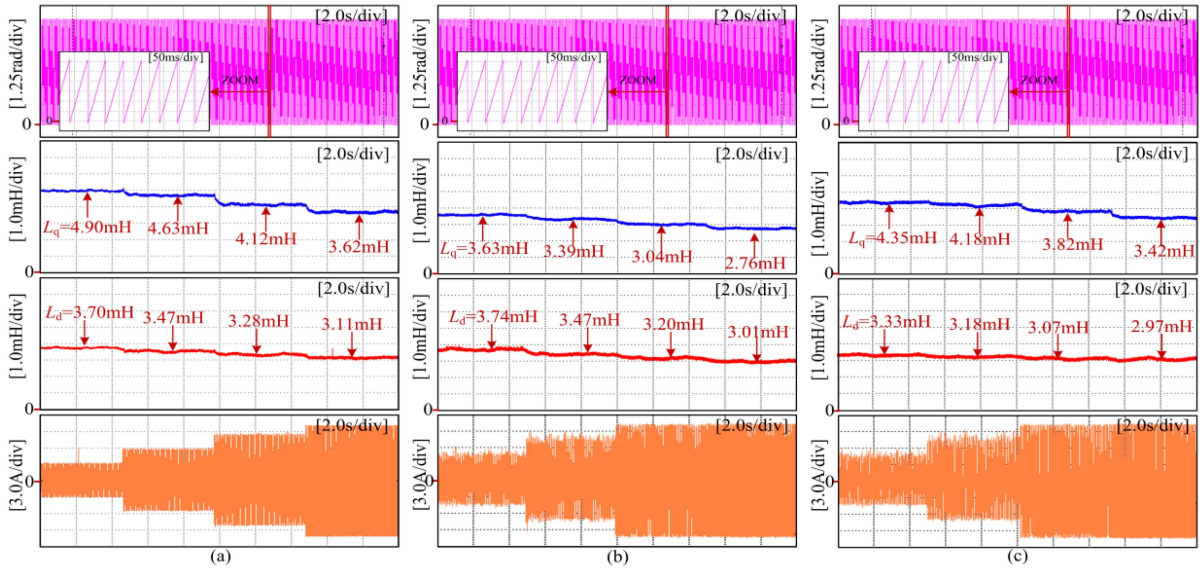

Fig. 13. Experimental results of inductance at 200r/min, $T_{e\_\mathrm{ref}} = 2$ N·m,4 N·m,6 N·m, 8 N·m. (a) Inductance identification based on HF signal amplitude. (b) Inductance identification based on HF signal amplitude and phase. (c) Proposed method.

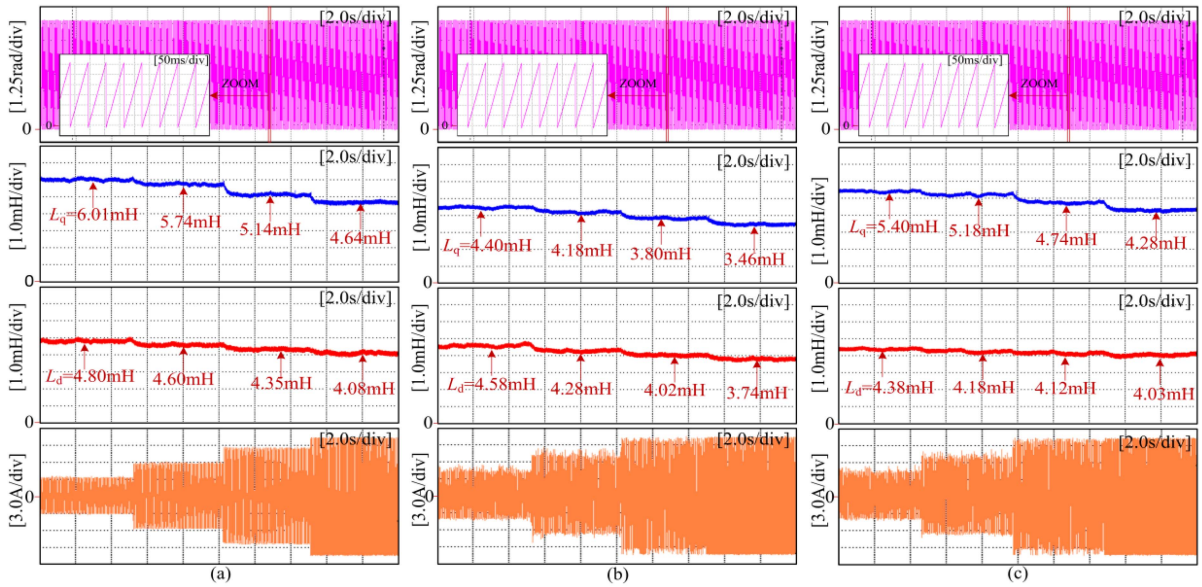

Fig. 14. Experimental results of inductance at 200 r/min with 1mH inductance in series, $T_{e\_\mathrm{ref}} = 2$ N·m, 4 N·m, 6 N·m, 8 N·m. (a) Inductance identification based on HF signal amplitude. (b) Inductance identification based on HF signal amplitude and phase. (c) Proposed method.

Different from the fundamental wave voltage, which behaves as a direct current, the injected HF voltage signal behaves as an alternating current in the *dq* coordinate system. Therefore, whether there is a difference in the mechanism of the effect of the digital control delay on the HF voltage signal needs to be analyzed in detail.

More generally, the injected HF voltage is written in the form of a complex vector as follows:

$$\begin{aligned}\boldsymbol{u}_{dqh\_\mathrm{inj}} &= u_{dh\_\mathrm{inj}} + j u_{qh\_\mathrm{inj}} \\ &= U_{h\_\mathrm{inj}} \cos(\omega_h t + \gamma_{\mathrm{inj}}) + \mathrm{j} U_{h\_\mathrm{inj}} \sin(\omega_h t + \gamma_{\mathrm{inj}})\end{aligned} \tag{26}$$

where U_{h_inj} is the amplitude of the HF voltage signal injected into the *d*- and *q*-axis; γ_{inj} is the initial phase angle of the HF voltage signal injected into the *d*- and *q*-axis; and ω_h is the frequency of the HF voltage signal.

Fig. 5 shows the variation of the HF voltage vector $\boldsymbol{u}_{dqh\_\mathrm{inj}}$ and the *dq* coordinate system during two consecutive control cycles. Due to the digital control, the HF voltage vector $\boldsymbol{u}_{dqh\_\mathrm{inj}}$ injected into the *dq* coordinate system at moment 0 can only act on the motor at the beginning of the next control cycle (moment T_s), and in the process the *dq* coordinate system changes counterclockwise the angle $\omega_e T_s$, Meanwhile at the moment T_s, the injected HF voltage vector $\boldsymbol{u}_{dqh\_\mathrm{inj}}$ is rotated counterclockwise by an angle $\omega_h T_s$, Therefore, the relationship

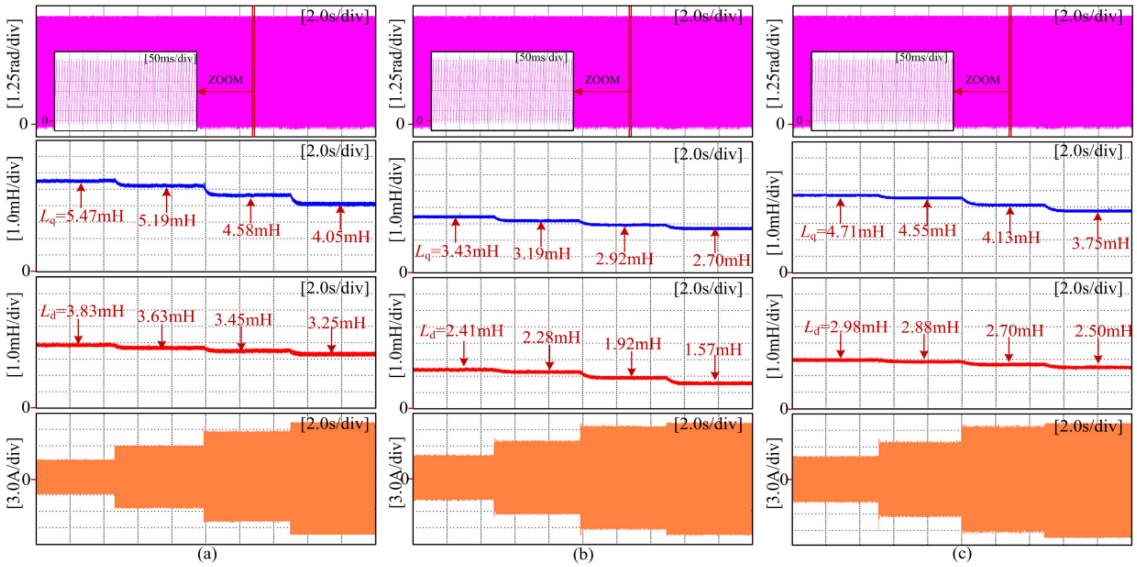

Fig. 15. Experimental results of inductance at 1200r/min, $T_{\mathrm{e\_ref}} = 2$ N·m, 4 N·m, 6 N·m, 8 N·m. (a) inductance identification based on HF signal amplitude. (b) Inductance identification based on HF signal amplitude and phase. (c) Proposed method.

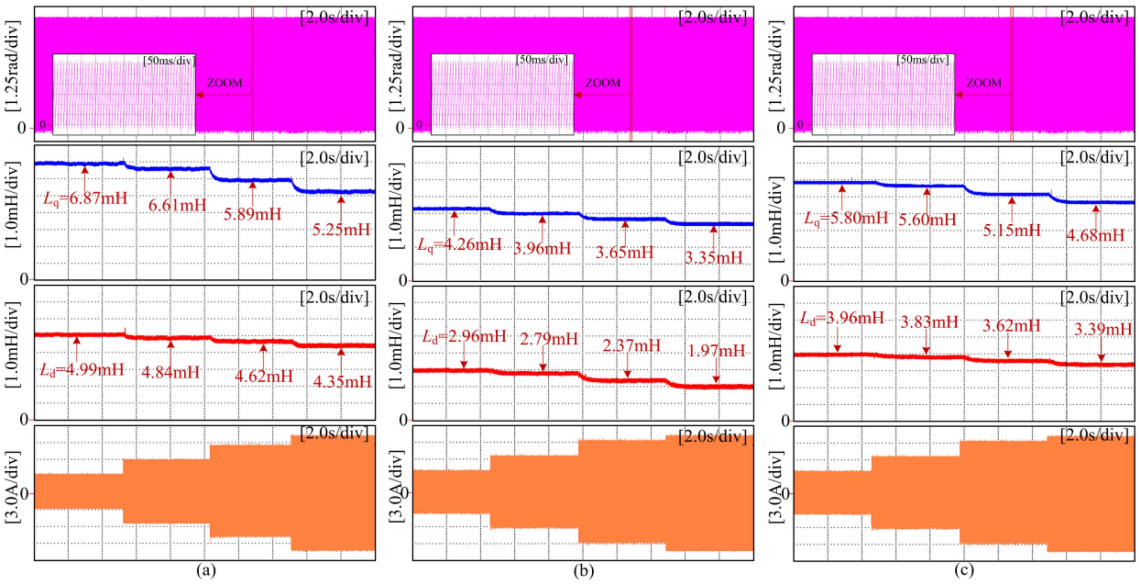

Fig. 16. Experimental results of inductance at 1200 r/min with 1mH inductance in series, $T_{\mathrm{e\_ref}} = 2$ N·m, 4 N·m, 6 N·m, 8 N·m. (a) Inductance identification based on HF signal amplitude. (b) Inductance identification based on HF signal amplitude and phase. (c) Proposed method.

between the injected HF voltage vector and the voltage vector acting on the motor terminal at the moment of Ts can be expressed as

$$\boldsymbol{u}_{dqh(Ts)} = \boldsymbol{u}_{dqh\_\mathrm{inj}(Ts)} e^{-j\omega_h T_s} e^{-j\omega_e T_s}. \tag{27}$$

The average HF voltage vector can be approximated as the HF voltage vector acting on the motor terminal during the time period from T_s to $2T_s$, let the average HF voltage vector be

$$\boldsymbol{u}_{dqh\_av} = u_{dh\_av} + j u_{qh\_av}. \tag{28}$$

The relationship between the average HF voltage vector and the voltage vector acting on the motor terminal at the moment of T_s can be expressed as follows:

$$\begin{aligned} \boldsymbol{u}_{\mathrm{dqh\_av}} &= \frac{1}{T_s}\int_{T_s}^{2T_s} \boldsymbol{u}_{dqh(Ts)} \cdot e^{-j\omega_e(\tau - T_s)} d\tau \\ &= \frac{2\sin(0.5\omega_e T_s)}{\omega_e T_s} \mathrm{e}^{-\mathrm{j}(0.5\omega_e T_s)} \boldsymbol{u}_{dqh(T_s)}. \end{aligned} \tag{29}$$

Consequently, by combining (26) and (29), the relationship between the injected HF voltage vector and the average voltage vector acting on the motor terminals during the time period from

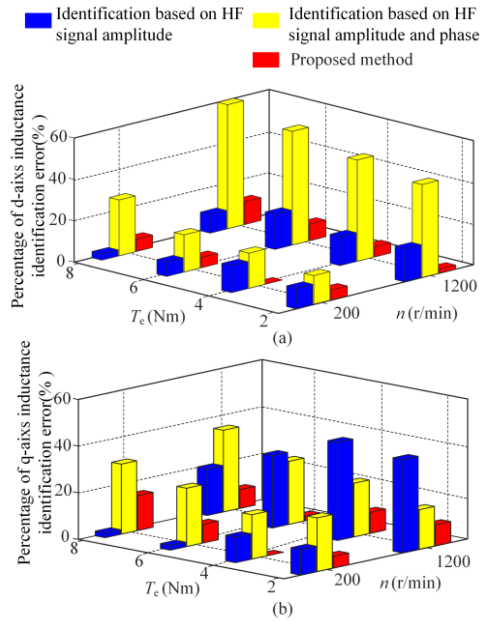

Fig. 17. Comparison of the error of identification results of string inductance. (a) d-axis inductance error percentage. (b) q-axis inductance error percentage.

T_s to $2T_s$ can be obtained as follows:

$$\boldsymbol{u}_{dqh\_av} = \frac{2\sin(0.5\omega_e T_s)}{\omega_e T_s} e^{-j(1.5\omega_e T_s)} \mathrm{e}^{-j\omega_h T_s} \boldsymbol{u}_{dqh\_\mathrm{inj}(T_s)}. \tag{30}$$

Therefore, in order to keep the actual HF voltage added to the motor terminal and the injected HF voltage consistent, a compensation for the injected HF voltage is required,according to (30), the expression for the compensated HF voltage is as follows:

$$\begin{cases} u_{dh\_\mathrm{com}} = m\left\{u_{dh\_\mathrm{inj}} \cos\left[(1.5\omega_e + \omega_h)T_s\right] \right. \\ \quad \left. -u_{qh\_\mathrm{inj}} \sin\left[(1.5\omega_e + \omega_h)T_s\right]\right\} \\ u_{qh\_\mathrm{com}} = m\left\{u_{d\_\mathrm{inj}} \sin\left[(1.5\omega_e + \omega_h)T_s\right] \right. \\ \quad \left. +u_{q\_\mathrm{inj}} \cos\left[(1.5\omega_e + \omega_h)T_s\right]\right. \end{cases} \tag{31}$$

where u_{dh_com} and u_{qh_com} are the compensated HF voltages.

Comparing (24) and (31), shows that the digital control delay has a different effect on the HF voltage in the dq coordinate system than the effect on the fundamental voltage, therefore, the injected HF voltage needs to be compensated by (31) during the parameter identification process in order to realize the accurate identification of the parameters.

In addition, when the motor control program is set to perform current sampling at the end of a control cycle, the HF current acquired at the moment of T_s will overshoot the average voltage vector acting on the HF current generated by the motor at an angle of $0.5\omega_h T_s$. The relationship between the HF current obtained from sampling at the moment of T_s and the HF response current produced by the motor when the average voltage vector is applied is shown in Fig. 6. Therefore, in order to accurately obtain the corresponding HF response current when the average voltage vector is in action, the HF current characteristics

TABLE I
PARAMETERS OF IPMSM

Parameter	Symbol	Value	Unit
Pairs of poles	n_p	5	--
Permanent magnet flux	λ_f	0.088	Wb
Phase resistance	R	0.4	Ω
d-axis inductance	L_d	3.0	mH
q-axis inductance	L_q	4.0	mH
Rated voltage	U_N	200	V
Rated torque	T_N	9	Nm
Rated voltage	N	2000	r/min

extracted in Section III-B need to be compensated as follows:

$$\begin{cases} I_{dh}\cos\mu_{d\_\mathrm{com}} = I_{dh}\cos\mu_d\cos\left(0.5T_s\omega_h\right) \\ -I_{dh}\sin\mu_d\sin\left(0.5T_s\omega_h\right) \\ I_{qh}\cos\mu_{q\_\mathrm{com}} = I_{qh}\cos\mu_q\cos\left(0.5T_s\omega_h\right) \\ -I_{qh}\sin\mu_q\sin\left(0.5T_s\omega_h\right) \\ I_{dh}\sin\mu_{d\_\mathrm{com}} = I_{dh}\sin\mu_d\cos\left(0.5T_s\omega_h\right) \\ +I_{dh}\cos\mu_d\sin\left(0.5T_s\omega_h\right) \\ I_{qh}\sin\mu_{q\_\mathrm{com}} = I_{qh}\sin\mu_q\cos\left(0.5T_s\omega_h\right) \\ +I_{qh}\cos\mu_q\sin\left(0.5T_s\omega_h\right) \end{cases}. \tag{32}$$

The block diagram of the proposed inductance identification structure based on the acquisition of HF response current and HF voltage characteristics is shown in Fig. 7.

V. EXPERIMENTAL RESULTS

A. Simulation Verification of the Effectiveness of Digital Control Delay Compensation

In order to verify the effectiveness of the compensation method proposed in this article, the following simulations are-carried out through the MATLAB/Simulink platform. When the motor torque is 6 N·m and the rotational speed is 1200 r/min, the results of the HF voltage characteristics that actually act on the motor terminal, the HF voltage characteristics without considering the delay compensation, and the HF voltage characteristics with considering the delay compensation are shown in Fig. 8. From the figure, shows that the compensated HF voltage characteristics are closer to the HF voltage characteristics acting on the motor terminal, while the HF voltage characteristics without considering the control delay are far away from the real value.

In order to further validate the effect of HF voltage characteristics accuracy on inductance identification results, Simulation verification of inductance identification was carried out at motor torque of 6 N·m and speeds of 200 and 1200 r/min. As shown in Fig. 9. From the figure, this shows that inductance value identified with the compensated HF voltage characteristics is closer to the real inductance value.

TABLE II
IDENTIFICATION RESULTS OF SERIES INDUCTANCE (*Q*-AXIS)

	Identification based on HF signals amplitude				Identification based on HF signals amplitude and phase				Proposed method			
L(mH)	2Nm	4Nm	6Nm	8Nm	2Nm	4Nm	6Nm	8Nm	2Nm	4Nm	6Nm	8Nm
200r/min	1.11	1.11	1.02	1.02	0.77	0.79	0.76	0.70	1.05	1.00	0.92	0.86
1200r/min	1.40	1.42	1.31	1.20	0.83	0.77	0.73	0.65	1.09	1.05	1.02	0.93

TABLE III
IDENTIFICATION RESULTS OF SERIES INDUCTANCE (*D*-AXIS)

	Identification based on HF signals amplitude				Identification based on HF signals amplitude and phase				Proposed method			
L(mH)	2Nm	4Nm	6Nm	8Nm	2Nm	4Nm	6Nm	8Nm	2Nm	4Nm	6Nm	8Nm
200r/min	1.10	1.13	1.07	0.97	0.84	0.81	0.82	0.73	1.05	1.00	1.05	1.06
1200r/min	1.16	1.21	1.17	1.10	0.55	0.51	0.45	0.40	0.98	0.95	0.92	0.89

B. Experimental Validation of HF Current Characteristics Extraction

In order to verify the feasibility of the proposed method, an experimental system as shown in Fig. 10 was constructed and. the parameters of the IPMSM are given in Table I In the experimental system, TMS320F28335 is used for the control unit. The sampling frequency of the control system is 10 kHz, the control period is 100 μs, the dc-bus voltage is 200 V, the rated power of the motor under test is 2 kW, and the rated torque is 9 N·m. In the experiments, the *d*-axis is injected with HF cosine voltage signals of amplitude 10 V, and the *q*-axis is injected with HF sinusoidal voltage signals of amplitude 10 V.

Fig. 11 shows the *dq*-axis current waveforms and the corresponding FFT analysis results at a motor speed of 400 r/min and a torque of 4 N·m. From the figure shows that after injecting the HF signal, the amplitude of the HF current in the *d*-axis current is 0.78 A and the amplitude of the HF current in the *q*-axis current is1.42 A in the *dq* coordinate system. *d*-axis current is 0.78 A and the amplitude of the HF current in the *q*-axis current is1.42 A in the *dq* coordinate system. Fig. 12 shows the results of the HF current characteristics extracted through the method proposed in this article and the results of the HF current amplitude synthesized from the HF current characteristics. From the figure, shows that the extracted HF current amplitudes in *d* and *q* axes are 0.75 A and 1.43 A. The results in Figs. 11 and 12 show that the proposed method in this article can accurately extract the characteristics of the HF response current.

C. Experimental Validation of Parameter Identification Results

In order to verify the accuracy of the inductance obtained by the method proposed in this article, the following experiments are conducted in this article. First, the proposed method in this article is validated at motor speeds of 200 r/min, 1200 r/min, and torques of 2 N·m, 4 N·m, 6 N·m, and 8 N·m. The article also reproduces the traditional inductor identification method based on the acquisition of HF signal amplitude information and the inductor identification method based on the acquisition of HF signal amplitude and phase angle, which are used as comparative validation, and the experimental results are shown in Figs. 13 and 15. From the experimental results, the differences in the results of the three methods can be shown, especially in inductor recognized based on the amplitude of the HF signal and the phase acquisition, due to the recognition results without considering the digital control delay and the other two methods of the results obtained there are obvious differences, but also from the side of the necessity to consider the digital control delay.

In order to compare the accuracy of the inductance obtained by the three methods of identification. The article also carries out the following experiments, three inductors with inductance value of 1mH and rated current of 50A (much larger than the rated current of the motor 10A) are connected in series to the motor system, and the total inductance in the newly composed system is recognized by three methods in the same motor operating conditions. The identification results are shown in Figs. 14 and 16. The inductance results identified in Figs. 13 and 14 and Figs. 15 and 16 are made differential, and the difference is the identification result of the series inductance, as given in Tables II and III.

Meanwhile, in order to visualize the accuracy of the inductance discrimination, an error histogram was plotted as shown in Fig. 17. From Tables II, III and Fig. 17, shows that the inductance identified by the proposed method in this article has two traditional methods have large errors. The inductance obtained by the proposed method in this article is recognized with better accuracy.

VI. CONCLUSION

For improving the accuracy of parameter identification based on HF signal injection, this article develops a strategy to accurately acquire HF voltage and HF current information. The content is mainly reflected in the followings.

1) Proposed an inductance identification method based on the acquisition of HF response current and HF voltage characteristics. The method establishes an inductance identification matrix with respect to HF voltage characteristics and HF current characteristics, considering the effects of stator resistance and cross-coupling, and the accurate acquisition of HF current characteristics is realized by

multifrequency rotational coordinate transformation in the ABC coordinate system.

2) Analyzes the mechanism of the digital control delay on the injected HF voltage and the sampled HF current signal, and proposes a digital control delay compensation strategy for the HF voltage.
3) The inductance identification results under the proposed method and the traditional two methods are obtained through experiments and the accuracy of the inductance obtained by recognizing the inductance by the method proposed in this article is verified by stringing in external inductance.

REFERENCES

[1] L. Sun, X. Li, and L. Chen, "Motor speed control with convex optimization-based position estimation in the current loop," *IEEE Trans. Power Electron.*, vol. 36, no. 9, pp. 10906–10919, Sep. 2021.

[2] L. Qu, W. Qiao, and L. Qu, "Active-disturbance-rejection-based sliding-mode current control for permanent-magnet synchronous motors," *IEEE Trans. Power Electron.*, vol. 36, no. 1, pp. 751–760, Jan. 2021.

[3] Z. Chen, S. Jin, Y. Shen, Y. Ma, X. Mao, and T. Shi, "Maximum efficiency per torque control of IPMSM based on loss criterion acquisition," *IEEE Trans. Power Electron.*, vol. 39, no. 11, pp. 14107–14117, Nov. 2024.

[4] Z. Chen, S. Jin, Y. Shen, and M. Wang, "Loss minimum control of surface permanent magnet synchronous motor based on virtual complementary square wave signal injection," *IEEE Trans. Emerg. Sel. Topics Power Electron.*, to be published, doi: 10.1109/JESTPE.2025.3538598.

[5] K. Liu and Z. Q. Zhu, "Online estimation of the rotor flux linkage and voltage-source inverter nonlinearity in permanent magnet synchronous machine drives," *IEEE Trans. Power Electron.*, vol. 29, no. 1, pp. 418–427, Jan. 2014.

[6] R. Raja, T. Sebastian, and M. Wang, "Online stator inductance estimation for permanent magnet motors using PWM excitation," *IEEE Trans. Transp. Electrific.*, vol. 5, no. 1, pp. 107–117, Mar. 2019.

[7] X. Yang, J. Zhan, Y. Shen, P. Liu, L. Guo, and Z. Zhang, "Parameter identification for SPMSM based on a superior ROA," *IEEE Trans. Power Electron.*, vol. 40, no. 6, pp. 7615–7627, Jun. 2025, doi: 10.1109/TPEL.2025.3534412.

[8] Y. Yu et al., "Full parameter estimation for permanent magnet synchronous motors," *IEEE Trans. Ind. Electron.*, vol. 69, no. 5, pp. 4376–4386, May 2022.

[9] Y. Yu, X. Huang, and Z. Li, "Overall electrical parameters identification for IPMSMs using current derivative to avoid rank deficiency," *IEEE Trans. Ind. Electron.*, vol. 70, no. 7, pp. 7515–7520, Jul. 2023.

[10] Y. Shen, D. Liu, P. Liu, X. Yang, and X. Yuan, "Error self-calibration of phase current reconstruction based on random pulsewidth modulation," *IEEE J. Emerg. Sel. Topics Power Electron.*, vol. 10, no. 6, pp. 7502–7513, Dec. 2022.

[11] S. Xiao and A. Griffo, "PWM-based flux linkage and rotor temperature estimations for permanent magnet synchronous machines," *IEEE Trans. Power Electron.*, vol. 35, no. 6, pp. 6061–6069, Jun. 2020.

[12] Z. Liu, W. Kong, X. Fan, and R. Qu, "Online multi-parameter observation of IPM machine with reconstructed nonlinear small-signal model based on dual EKF," *IEEE Trans. Ind. Electron.*, vol. 71, no. 2, pp. 1234–1245, Feb. 2024.

[13] Y. Wang et al., "A robust DPCC for IPMSM based on a full parameter identification method," *IEEE Trans. Ind. Electron.*, vol. 70, no. 8, pp. 7695–7705, Aug. 2023.

[14] J. Zhou, K. Huang, S. Huang, S. Liu, H. Zhao, and M. Shen, "Inductance parameter identification method of permanent magnet synchronous motor based on the HF rotating square wave voltage injection," in *Proc. 22nd Int. Conf. Elect. Mach. Syst.*, 2019, pp. 1–4.

[15] G. Feng, C. Lai, K. Mukherjee, and N. C. Kar, "Current injection-based online parameter and VSI nonlinearity estimation for PMSM drives using current and voltage DC components," *IEEE Trans. Transp. Electrific.*, vol. 2, no. 2, pp. 119–128, Jun. 2016.

[16] M. Martinez, D. Reigosa, D. Fernández, J. M. Guerrero, and F. Briz, "Enhancement of permanent-magnet synchronous machines torque estimation using pulsating high-frequency current injection," *IEEE Trans. Ind. Appl.*, vol. 56, no. 1, pp. 358–366, Jan./Feb. 2020.

[17] S. El Daoudi, L. Lazrak, and M. A. Lafkih, "Sliding mode approach applied to sensorless direct torque control of cage asynchronous motor via multi-level inverter," *Protection Control Modern Power Syst.*, vol. 5, no. 1, pp. 1–10, Apr. 2020.

[18] D. Reigosa, D. Fernández, M. Martínez, J. M. Guerrero, A. B. Diez, and F. Briz, "Magnet temperature estimation in permanent magnet synchronous machines using the high frequency inductance," *IEEE Trans. Ind. Appl.*, vol. 55, no. 3, pp. 2750–2757, May/Jun. 2019.

[19] S. Kang, D. Reigosa, B. Sarlioglu, and R. D. Lorenz, "D-and q-axis inductance estimation and self-sensing condition monitoring using 45° angle high-frequency injection," *IEEE Trans. Ind. Appl.*, vol. 57, no. 1, pp. 506–515, Jan./Feb. 2021.

[20] K. Yu and Z. Wang, "Online decoupled multi-parameter identification of dual three-phase IPMSM under position-offset and HF signal injection," *IEEE Trans. Ind. Electron.*, vol. 71, no. 4, pp. 3429–3440, Apr. 2024.

[21] Y. Wang, Y. Xu, and J. Zou, "Online multiparameter identification method for sensorless control of SPMSM," *IEEE Trans. Power Electron.*, vol. 35, no. 10, pp. 10601–10613, Oct. 2020.

[22] Q. Wang, G. Wang, N. Zhao, G. Zhang, Q. Cui, and D. Xu, "An impedance model-based multiparameter identification method of PMSM for both offline and online conditions," *IEEE Trans. Power Electron.*, vol. 36, no. 1, pp. 727–738, Jan. 2021.

[23] Z. Liu, X. Fan, W. Kong, L. Cao, and R. Qu, "Improved small-signal injection-based online multiparameter identification method for IPM machines considering cross-coupling magnetic saturation," *IEEE Trans. Power Electron.*, vol. 37, no. 12, pp. 14362–14374, Dec. 2022.

[24] S. Liu et al., "Virtual-axis injection based online parameter identification of PMSM considering cross coupling and saturation effects," *IEEE Trans. Power Electron.*, vol. 38, no. 5, pp. 5791–5802, May 2023.

[25] G. Wang et al., "Self-commissioning of permanent magnet synchronous machine drives at standstill considering inverter nonlinearities," *IEEE Trans. Power Electron.*, vol. 29, no. 12, pp. 6615–6627, Dec. 2014.

[26] A. Namdar, "A robust principal component analysis-based approach for detection of a stator inter-turn fault in induction motors," *Protection Control Modern Power Syst.*, vol. 7, no. 4, pp. 1–24, Jul. 2022.

[27] Q. Wang, G. Zhang, G. Wang, C. Li, and D. Xu, "Offline parameter self-learning method for general-purpose PMSM drives with estimation error compensation," *IEEE Trans. Power Electron.*, vol. 34, no. 11, pp. 11103–11115, Nov. 2019.

[28] Q. Wang et al., "An offline parameter self-learning method considering inverter nonlinearity with zero-axis voltage," *IEEE Trans. Power Electron.*, vol. 36, no. 12, pp. 14098–14109, Dec. 2021.

[29] Q. Wang, G. Wang, S. Liu, G. Zhang, and D. Xu, "An inverter-nonlinearity-immune offline inductance identification method for PMSM drives based on equivalent impedance model," *IEEE Trans. Power Electron.*, vol. 37, no. 6, pp. 7100–7112, Jun. 2022.

[30] Z. Chen, Y. Yan, T. Shi, X. Gu, Z. Wang, and C. Xia, "An accurate virtual signal injection control for IPMSM with improved torque output and widen speed region," *IEEE Trans. Power Electron.*, vol. 36, no. 2, pp. 1941–1953, Feb. 2021.

Zhiwei Chen (Member, IEEE) was born in Pingdingshan, China, in 1994. He received the B.S. degree in electrical engineering from China University of Mining and Technology, Xuzhou, China, in 2017, and the Ph.D. degree in electrical engineering from Tianjin University, Tianjin, China, in 2023.

He is currently a Lecturer with the College of Electrical and Information Engineering, Zhengzhou University of Light Industry, Zhengzhou, China. His research interests include electrical machines, motor drives and power electronics.

Chaoyang Geng was born in Xuchang, China, in 2000. He received the B.S. degree in electrical engineering from Henan Institute of Science and Technology, Xinxiang, China, in 2023. He is currently working toward the M.S. degree in electrical engineering with Zhengzhou University of Light Industry, Zhengzhou, China.

His research interests include electrical machines, motor drives and power electronics.

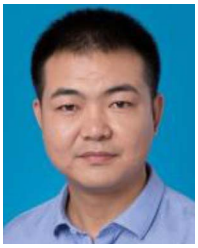

Yongpeng Shen (Member, IEEE) was born in Henan, China, in 1985. He received the M.S. degree in electrical engineering from Zhengzhou University of Light Industry, Zhengzhou, China, in 2010, and the Ph.D. degree in control science and engineering from Hunan University, Changsha, China, in 2015.

Since 2015, he has been with the Zhengzhou University of Light Industry and Henan Key Lab of Information-based Electrical Appliances. Since 2021, he has been with the National Engineering Laboratory for Robot Visual Perception and Control Technology, Changsha, Hunan, China. His research interests include management, control and optimization of electric and hybrid electric vehicle components.

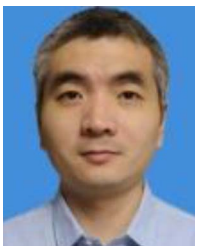

Mingjie Wang received the B.E. degree in electrical engineering from Henan Polytechnic University, Jiaozuo, China, in 2004, and the M.S. and Ph.D. degrees in electrical engineering from Zhengzhou University, Zhengzhou, China, in 2007 and 2015, respectively,

He has been a Lecturer with the Department of Electrical Engineering, Zhengzhou University of Light Industry, Zhengzhou, since 2015. His research interests include modeling and design of PM machines, linear motor drives, and controls.

Xiaoliang Yang (Member, IEEE) was born in Hebei, China, in 1980. He received the B.S. and M.S. degrees in electrical engineering from Zhengzhou University of Light Industry, Zhengzhou, China, in 2003 and 2009, respectively, and the Ph.D. degree in control science and engineering from Hunan University, Changsha, China, in 2021.

He is currently an Associate Professor in electrical engineering with Zhengzhou University of Light Industry. His current research interests include wind power turbine control and motor control.